# NOISE PREDICTION FROM A LOW-MACH NUMBER AXIAL FAN WITH LES AND BEM

Sergei G. CHUMAKOV[1], Yoon Shik SHIN[2], Guillaume A. BRÈS[3],
Frank E. HAM[3], Joseph W. NICHOLS[4]

[1] *Research and Technology Center, Robert Bosch LLC,*
*4005 Miranda Ave, Palo Alto, CA 94304, U.S.A.*

[2] *Electrical Drives Division, Robert Bosch LLC,*
*101 First Ave, Waltham MA 02451, U.S.A.*

[3] *Cascade Technologies Inc., 2445 Faber Pl., Palo Alto, CA 94303, U.S.A.*

[4] *Department of Aerospace Engineering and Mechanics,*
*University of Minnesota, Minneapolis, MN 55455 U.S.A.*

## SUMMARY

A new approach to noise prediction is developed and is illustrated using the case of an engine cooling fan. The noise prediction problem is divided into capturing the noise sources in the flow and propagating the noise to observer locations, the latter being the subject of this paper. The air velocities and static pressures from the LES simulation of a rotating fan are recorded on a stationary permeable FWH surface that surrounds moving parts of geometry; later this surface is used as a radiating source input to the BEM acoustic projection. The developed combination of FWH and BEM approaches is implemented in massively parallel LES framework. The approach is validated with sound measurements from a fan in an anechoic chamber.

## INTRODUCTION

Computational prediction of noise is highly relevant in contemporary industrial environment. A good illustration of this thesis is the emerging importance of noise mitigation in the automotive industry. The general trend in recent years has been aggressive downsizing and higher packing density under the hood, and as a consequence, an increase in noise level. Historically the development of quieter fans relied heavily on the mixture of experience, intuitive expert knowledge and rapid prototyping with little or no involvement of computational fluid dynamics (CFD). However, recent advances in High Performance Computing (HPC) resulted in extremely powerful machines which are accessible to industrial engineers. Using such facilities makes CFD a feasible alternative to experimental trial-and-error methods in component development. Here we illustrate this on the problem of predicting noise generated by an engine cooling fan.

The noise prediction problem can be broadly separated into two parts: modeling noise generation and noise propagation. Combined prediction of both phenomena in the same CFD framework is

challenging because of the disparity in the strength of turbulent and acoustic flow features. Energy stored in acoustic waves is much lower than the energy of the turbulent flow. Using the same CFD code for the prediction of both can be detrimental for the accuracy of the noise propagation, because the numerical schemes that are used for the flow prediction can be too dissipative for accurate propagation of weak pressure waves, i.e., sound waves. Also the propagation of sound involves large length scales (meters) that, coupled with high resolution requirements for the flow modeling (fractions of a millimeter), results in calculations that become prohibitively expensive. Thus it seems natural to use two different solvers – the flow solver and the acoustic solver – to treat the two parts of the problem separately.

The noise generated by a fan consists of two components: broadband and tonal. While the tonal component is naturally more distinguishable (and annoying) to the human ear, the broadband component sets the overall noise pressure level and is just as important to predict. This poses some constraints on the flow solver. Currently available tools such as Reynolds-Averaged Navier Stokes (RANS) have the potential of predicting only the tonal component of noise. The reason for this is the inability of RANS to capture turbulent fluctuations in the inertial range of scales which produce the broadband noise. Thus a flow solver based on the Large Eddy Simulation (LES) approach, in which the most energetic (large) flow structures are resolved while the small flow structures are modeled, was determined to be a better fit. A detailed overview of the LES flow solver VIDA used in this work is provided in [1].

In this paper, we concentrate on a description of the acoustic solver which is used to propagate the noise generated by an engine cooling fan to an arbitrary microphone position. The noise propagation algorithm uses the Boundary Element Method framework; it is modified to account for sound reflections from arbitrary hard surfaces and is specifically targeted towards utilization of massively parallel HPC clusters.

## SIMULATION AND MEASUREMENTS SETUP

The configuration of the flow domain for the fan operation was chosen in such a way that the flow and sound simulations and the counter measurement of each – separate measurements for the flow field and the sound propagation – can be considered to be equivalent in terms of flow and acoustic conditions. The four different flow domain geometries are: the LES flow simulation domain, the index-matched PIV flow measurement facility, the BEM boundary geometry and the acoustic measurement setup.
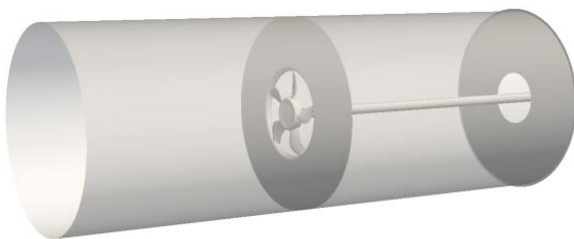


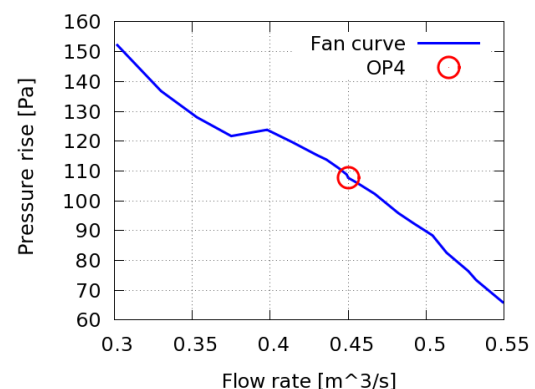*Figure 1: Schematic of the LES computational domain.*



*Figure 2: Fan performance curve and chosen operating point.*

A Bosch 5-blade axial fan was rotated with angular speed set at 2630 RPM with the volumetric flow rate of 0.45 m3/s, which resulted in the measured pressure rise across the fan of approximately 110 Pa. The operating point is referred to as "operating point 4" (OP4). This particular operating point was chosen for the validation of acoustic solver because it falls between "idle" and "ram-air"

regimes, and is atypical design point of for automotive cooling fans.  The fan operating point, along with the fan performance curve, is shown in the Figure 2.

The computational domain for LES was constructed using a 350 mm radius cylindrical duct that extended roughly 1 meter upstream and 1 meter downstream of the fan (See Figure 1). The significance of the upstream side extent of the duct was strategically different between each setup – for the LES computation domain and the PIV facility, the upstream duct was primarily a mean to provide controlled inflow condition for the fan. For the LES computation domain, the space is also used to attenuate the reflection of acoustic waves at the numerical boundary. For the BEM simulation and the acoustic measurement, the upstream duct geometry was a sound scattering structure which was in the way of sound generated by the fan and the measurement probes, meaning that matched geometry between two was crucial for the validation of the acoustic prediction. The acoustic measurement setup and the BEM geometry had a converging bell-mouth nozzle at the inlet in order to achieve uniform velocity profile for the fan inlet flow (see Figure 3).  The detailed description of the LES flow solver and its validation against the PIV experimental data is described in detail in complementary works [1,2].
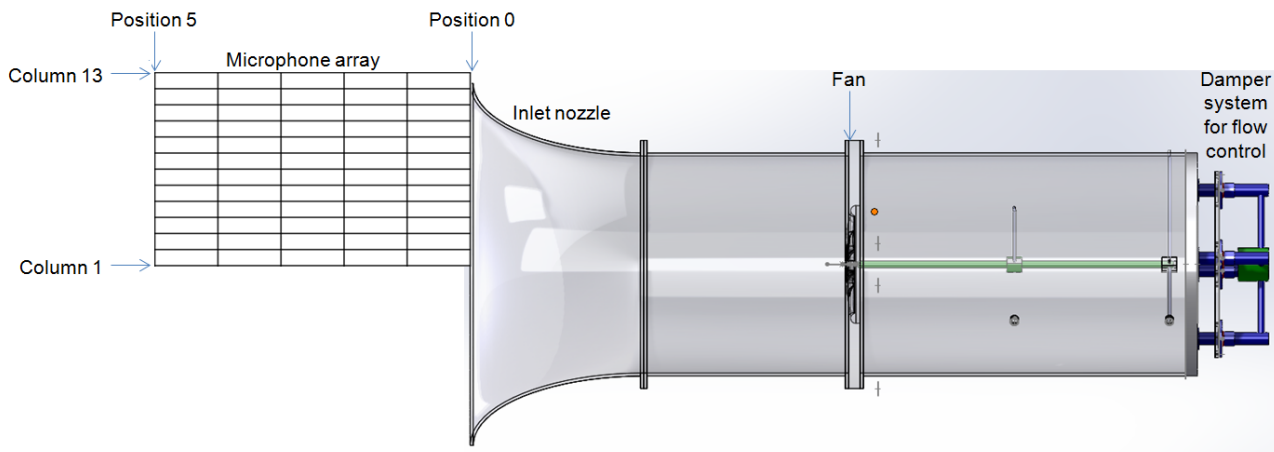


*Figure3: Schematic of the test rig in an anechoic chamber for acoustic measurements.*

The sound probe locations were distributed over the free space adjacent to the inlet bell-mouth. The number of points was chosen to provide sufficient spatial resolution for the scattering patterns resulting from the upstream duct geometry in a wide range of frequencies. The 13 (radial) by 6 (axial) points covered 0.61 m (radial) by 1 m (axial) area as shown in Figure 3. The driving motor for the acoustic measurement setup was placed outside of the discharge opening to keep the motor far from the fan and keep the motor noise below the fan noise level over the entire frequency range.

The size of the anechoic chamber was 15'×19'×12' with 150 Hz cut-off anechoic treatment. The 13 ICP type microphones were BSWA Technology MPA 201, and a B&K 4231 acoustical calibrator was used for 94 dB calibrations at 1 kHz. The data acquisition system was HEAD labV12 series. Sound of each steady-state fan operation was recorded for 20 seconds at 24 kHz sampling frequency. A single Fourier transform of the whole 20 seconds of sample was bin-averaged and weighted to calculate power spectral density with a 20 Hz resolution. For comparisons, the numerical results were treated in the same manner except for the length of the numerical data being shorter than the measurement.

## ACOUSTIC PROPAGATION APPROACH

For far-field noise predictions, the accurate propagation of the small amplitude acoustic fluctuations from the near-field source region to the far-field microphones within the computational domain would be prohibitively expensive. The Ffowcs Williams–Hawkings (FWH) equation [3] is one of the most commonly used methods to overcome this challenge. Sound at a far-field location can be

computed from flow information on an arbitrarily-shaped surface *S* and the volume-distributed sources outside of *S*. If *S* corresponds to a physical solid surface (e.g., a fan blade or an aircraft landing gear) the FWH formulation is referred to as solid (impenetrable), and as permeable (porous) otherwise. One advantage of the permeable formulation is that it allows for the acoustic sources in the volume outside the solid surface but inside the data surface *S* to be taken into account.
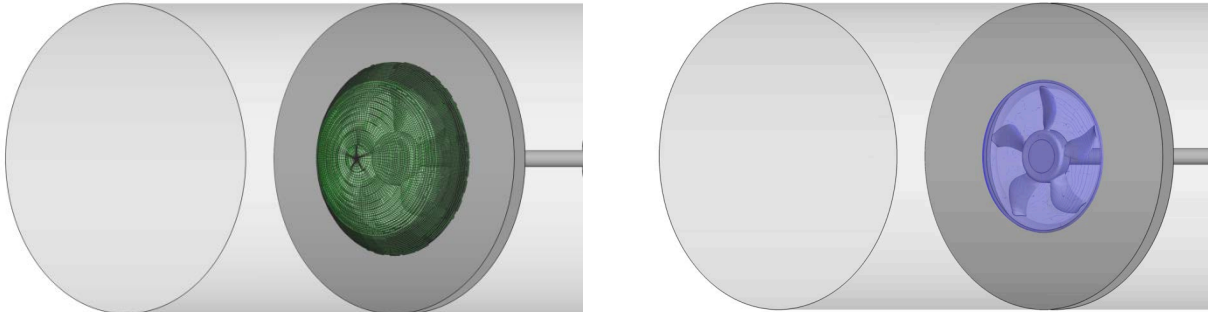


*Figure 4: Schematic of the fan setup and FWH surfaces S1 (left) and S5 (right)*

For the present fan configuration, several permeable surfaces were considered upstream of the fan, with different shapes and locations. Figure 4 shows two such surfaces, *S1* and *S5*. The surface *S1* consists of a spherical cap with radius of 25 cm. The center of the sphere is placed at the centerline, 10 cm downstream of the fan. The surface *S1* contains 26,000 panels which are faces of the computational mesh, and is placed in the region with medium mesh resolution. The surface *S5*, on the other hand, is located in the high resolution region close to the fan and has approximately 340,000 hexahedral panels matching the topology and resolution of the underlying LES grid, to ensure the accurate capture of the acoustic waves that propagate from the fan surface to the FWH surface by the flow solver. Processing the data from *S5* requires much more effort comparing to *S1*. However, when compared, the acoustic results from both surfaces were essentially equivalent, and we conclude that the resolution of *S1* is sufficient enough to capture the sound waves that pass through the FWH surface. Thus in this paper we only show the results from the surface *S1*.

While the LES flow solver uses a rotating reference frame to simulate the fan rotation, the pressure and three components of velocity are interpolated onto the FWH surface in a fixed laboratory frame. Since the distance between the noise sources (i.e., stationary surfaces *S1* or *S5*) and the observers (i.e., far-field microphones) is fixed and time-independent, there is no Doppler effect and an efficient frequency-domain permeable formulation [4] can be used. The formulation and its implementation in the LES framework from Cascade Inc. are discussed in detail in [5]. As the permeable FWH surface is designed to enclose the main noise sources region, the (computationally expensive) volume term can be assumed small and is neglected in the present calculations.

One of the underlying hypotheses of Ffowcs Williams–Hawkings equation is that the propagation of the acoustics waves is assumed to be in free space. Therefore, the reflections from the duct boundaries are neglected in the noise predictions directly from the FWH solver. Such predictions for observers outside of the bell-mouth are referred to as "FWH direct" in the remainder of the paper. To account for the effect of the duct on the sound radiation, a boundary element method (BEM) was implemented in the LES framework and efficiently coupled to the FWH solver.

Note that the direct FWH method is well-suited for parallelization, since the calculations for each surface element, each frequency and each observer are independent. The current MPI implementation is done in the same massively-parallel infrastructure than the flow solver. It uses a standard load-balancing approach on the FWH surface elements: each processor computes the noise contribution of only a portion of the surface, for all the observers and frequencies; the individual contributions are then recombined linearly as final output. This results in very efficient calculations, even for large number of time samples, surface elements and/or observers, as is the case with the BEM solver.

It is also important to highlight the difference between the proposed method and the Kirchhoff method. The latter assumes a solution of the linear wave equation on the chosen surface, and the noise prediction from the Kirchhoff method can change dramatically if this hypothesis is not satisfied. For a surface placed in a linear region, there is indeed no difference between the two approaches, and it has been shown that the FWH permeable surface formulation is equivalent to the linear Kirchhoff formulation, with addition of volume integral of quadrupoles [6,7]. However, in our case the surface *S1* is placed relatively close to the fan in order to be in the region with high enough mesh resolution. The distance between the top of the spherical cap to the hub center is about 15 cm, where nonlinear effects cannot be neglected. Thus by using the permeable FWH approach we avoid high sensitivity with respect to the choice of the control surface which is exhibited by the Kirchhoff method. This is crucial for the case of surfaces that are even closer to the fan (likely in the non-linear region) such as *S5*.

## DESCRIPTION OF BEM CODE

Simulation of low Mach number flows with acoustics is computationally challenging because the separation of aerodynamic and aeroacoustic scales leads to models consisting of stiff systems of partial differential equations. In other words, in these flows the propagation speed of the acoustics imposes severe time step restrictions that are otherwise unnecessary to accurately represent the aerodynamic part of the flow. Simulation methods for low Mach number flows with acoustics might be organized into three main categories.

The first approach is to treat the aerodynamic part of the flow as incompressible and apply the acoustic analogy arising from Lighthill's exact rearrangement of the compressible Navier-Stokes equations separating acoustic propagation from source terms [8]. The aerodynamic part of the calculation captures the acoustic source terms which then provide an input to the second phase of calculation where acoustic propagation is treated with a linear solver. In configurations without a homogeneous direction (involving complex geometry), a potential problem with this approach is that it entails saving large databases of 3D fields of the fluctuating source terms that are needed for the second stage of the calculation.

The second approach is to simply solve the fully compressible equations, with the downside of having a restrictive timestep. An advantage of this approach, however, is that since acoustic waves are supported throughout the domain, acoustic information can be collected on a surrounding 2D surface (rather than 3D) before being propagated to the far field [5]. Another advantage of this approach is strong parallel scalability owing to the hyperbolic nature of the underlying governing equations.

The third approach, representing the middle ground between the extremes of the first two, is to use a semi-implicit method whereby the acoustics are isolated and integrated in time using an implicit method, while the rest of the dynamics is treated explicitly. This leads to the solution of Helmholtz equation for the acoustic part of the pressure at every timestep, which relaxes the restriction on the maximum timestep, but at the same time maintains the presence of acoustic waves in the domain so that they may be recorded on a 2D surface. This third approach is the one taken in VIDA, the variable-density low Mach number solver, which is used to generate the input for acoustic solver in this work [1].

A key component to the prediction of low-Mach number sound is the propagation from either the 3D source region, or a 2D surface surrounding it (see Figure 4), to the far-field locations where microphones are located in the experiment. Because the acoustic wavelengths are much longer than the length scales of the turbulence associated with acoustics sources, it is not efficient to use LES to propagate sound over large distances. Since the propagation of most sound is well-represented by a linear process, one can use free-space Green's functions, with or without convection, to model this process. In the case of the automotive fan experiment, the fan is partially enclosed by a lengthy

inlet duct with bell mouth as shown in Figure 3, with microphones positioned outside. One could theoretically place the FWH surface at the inlet of the duct, which would require detailed computation of the flow in the entire flow domain. An alternative is to place the FWH surface close to the source-containing region, as is done with *S1*, and model the scattering effect of the duct by a boundary element method (BEM) [9].

While it is important to capture the effects of acoustic reflections from the solid wall of the inlet duct, it is equally important that the method does not spuriously create reflections where none should exist. In Figure 4 the upstream boundary is a flat disc at the inlet duct entrance, through which the acoustic waves must pass with minimal reflection. Numerical boundary conditions invariably lead to a small amount of reflection, although this can be minimized using specialized numerical schemes [10,11]. For low-Mach number solvers, special care must be taken to ensure consistency between the prediction step and the Helmholtz solver, since there is no diagnostic equation for pressure. Numerical sponge layers present an attractive solution where acoustic waves are damped slowly as they approach the boundary [12].

## RESULTS AND DISCUSSION

In this section we present results of post-processing the data from LES simulation of a flow around a 5-blade axial fan at 2630 RPM. The pressure and velocity data were recorded on the surface S1 over the course of about 0.44 s with time step of 5E-5 sec. This results in approximately 8800 samples with the sampling rate of 20 kHz.

### Comparison between direct FWH and FWH+BEM

For application of the BEM approach, the upstream portion of the cylinder and the bell-mouth were discretized as a set of rectangular panels with dimensions roughly $1.6 \times 1.6$ cm, referred to as "fine". To look into the BEM convergence process, we ran another noise calculation with coarser discretization (referred to as "coarse") with panel size about $3.2 \times 3.2$ cm. The fine resolution resulted in about $N$=20,000 BEM panels, and the coarse resolution produced $N$=5000 panels. The number of frequencies was determined to be 4,390 from the length of the simulation. To apply the BEM algorithm, a linear dense complex matrix system of rank $N$ had to be solved for every considered frequency. Thus, if we apply a simple Gaussian elimination to solve linear systems, the cost of the acoustic computation scales linearly with the number of considered frequencies and cubically with the number of BEM panels.
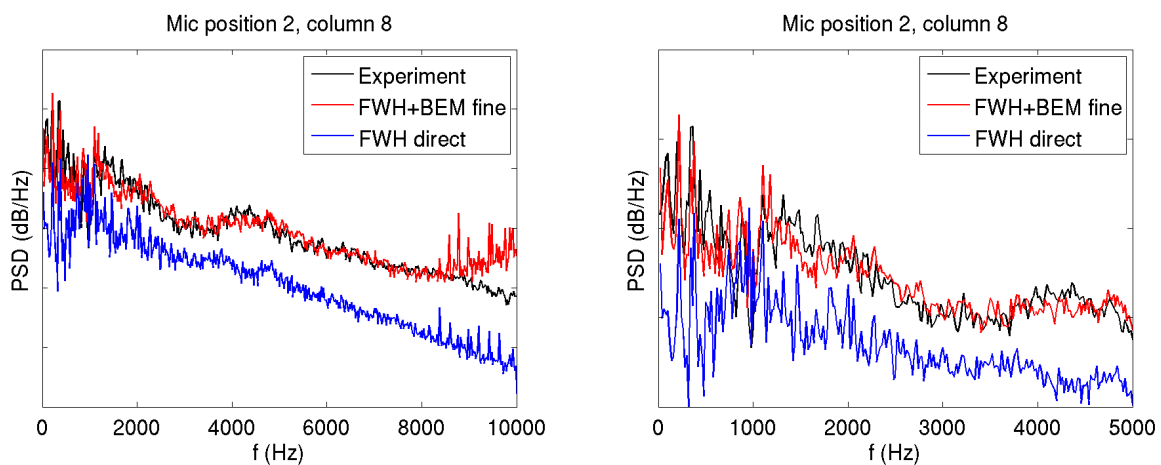


*Figure 5: Comparison of measured and computed fan noise spectra for microphone at position 2, column 8, for frequency up to 10 kHz (left) and 5kHz (right)*

Figure 5 shows comparison between experimental measurements in anechoic chamber, FWH direct prediction and FWH+BEM prediction, for a fixed microphone position. The left panel shows the

spectra comparison for up to 10 kHz, while the right panel shows comparison for spectra up to 5 kHz. The distance between ticks on Y-axis is 10 dB/Hz. The figures show that FWH+BEM combination is able to match the overall trends across the frequencies and the magnitude of the major peaks in the low-frequency range with very good accuracy.

It is evident from the figures that reflections play an important role in the overall sound characteristics. The difference between direct FWH and FWH+BEM spectra is close to 10 dB/Hz, which is especially evident in high-frequency range. This is expected and can be roughly explained by the focusing effect of the pipe and bell-mouth. If we approximate the fan as a point source and take a ratio of solid angles that receive acoustic energy from this source for in case of scattering surface and direct propagation, we obtain that the average increase of sound level should be equal to approximately 9.33 dB.

**Effect of BEM panel size**

It is worth noting that with panels of the size of 1.6 cm$^2$ one naturally expects the minimum resolved wave length to be about 9.6 cm, or 6 panel dimensions. Thus a reasonable match between experiment and model should not extend beyond 3.4 kHz. However, Figure 5 shows that in our case the range of a reasonably good match between experiment and FWH+BEM results extends to about 8 kHz. It appears that for this particular configuration it might be sufficient to have less than 6 panels per wavelength of interest.
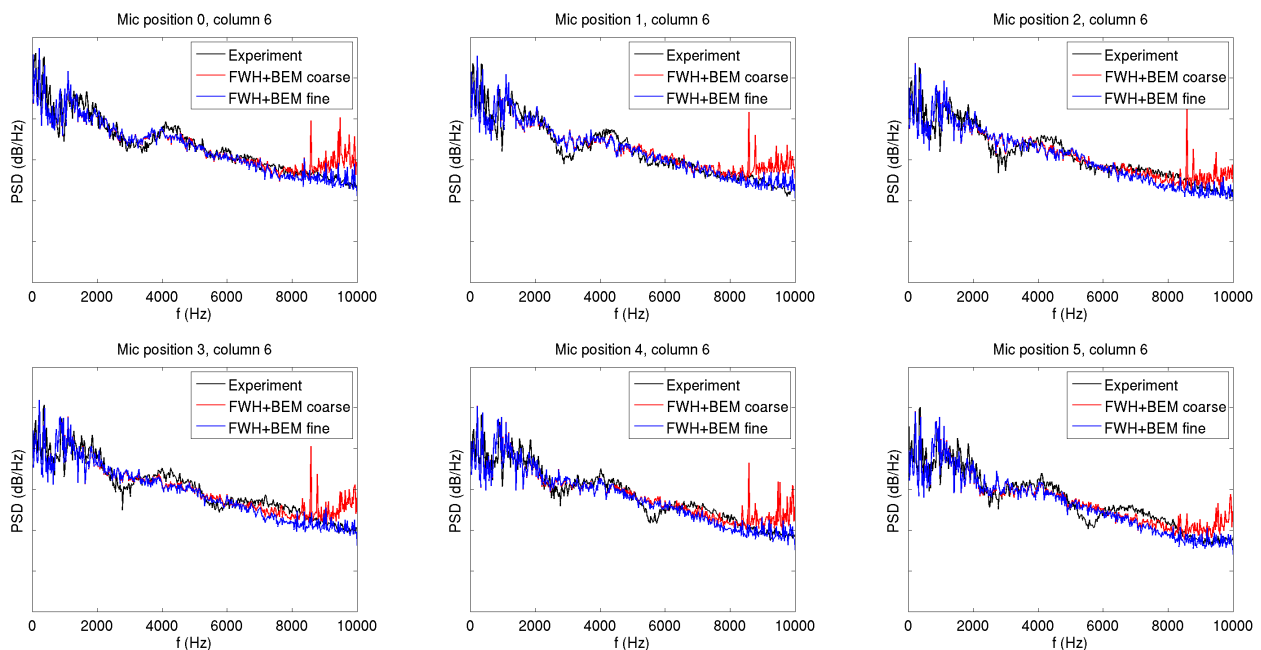


*Figure 6: Comparison of two BEM resolutions for all microphones in column 6: spectra up to 10 kHz*

In order to further investigate the effects of BEM resolution we compared results from two FWH+BEM runs with different BEM panel size, "coarse" and "fine". The results are shown in the Figures 6 and 7 for frequency ranges of up to 10 kHz and 5 kHz, respectively. Shown are spectra for all microphones from the column 6 (data from other columns produce similar results).

The plots show that there is no noticeable difference between the computed spectra for frequencies lower than 6 kHz, and when zoomed into the range of up to 5 kHz, the spectra are virtually identical. Thus we can conclude that for our particular configuration one can obtain good approximation for the spectra even with very coarse BEM discretization (the coarse case has 2.1 panels per wavelength of frequency 5 kHz). This can be attributed to the smoothness of the

reflecting surfaces and to the fact that they do not possess geometrical features that are comparable in size to the high-frequency wavelengths.
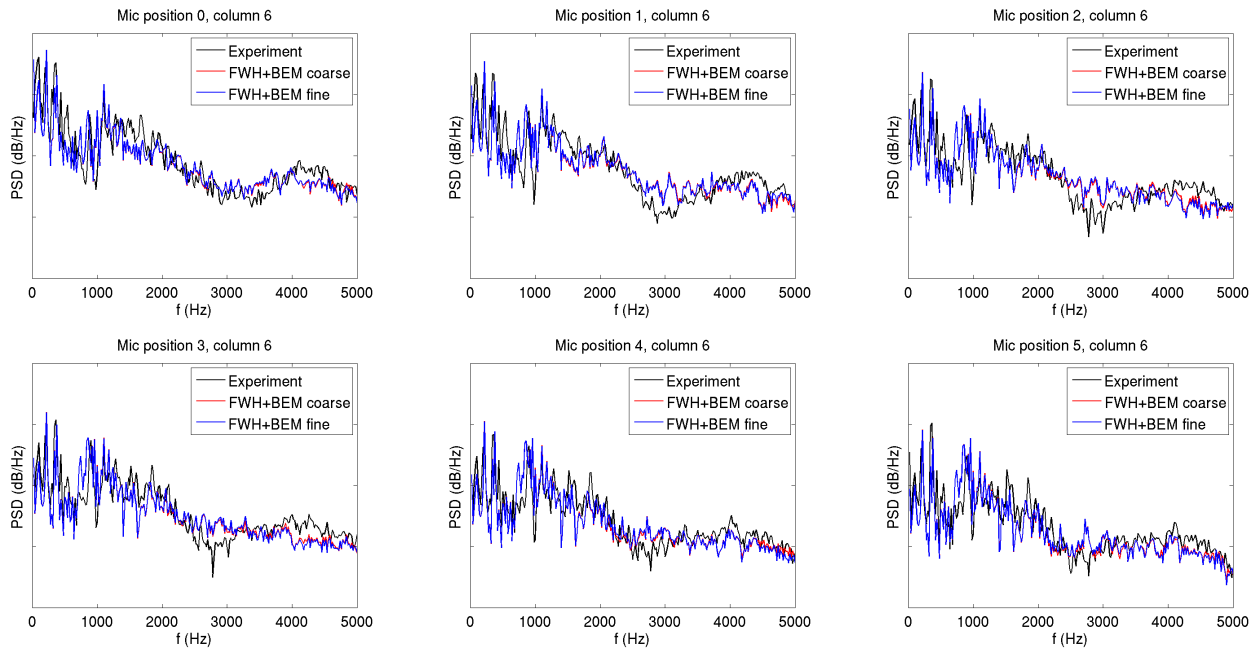


*Figure 7: Comparison of two BEM resolutions for all microphones in column 6: spectra up to 5 kHz.*

## Color maps of the sound field

To further evaluate the quality of prediction for our method, we show colormaps for three wave bands (300-400 Hz, 500-600 Hz and 3000-3300 Hz). Figures 8 through 10 show comparison between computed and measured sound pressure levels. The color scale has units of dB/Hz because the bin width changes from 100Hz to 300Hz and thus plotting the spectral density is more informative than plotting the total bin power.

Overall, the figures show that the LES+FWH+BEM method exhibits a good accuracy in prediction of the sound power level over the entire spectrum.
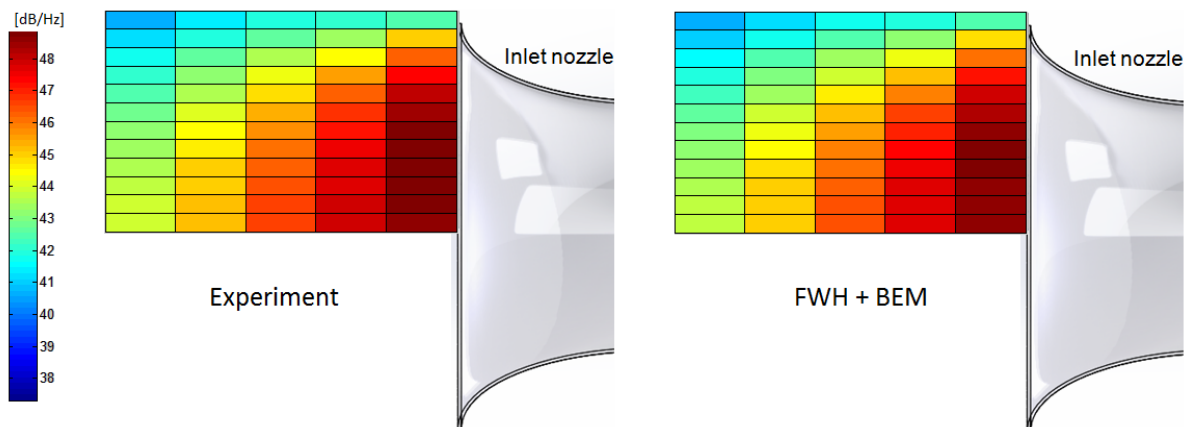


*Figure 8: Comparison of color maps from experiment and LES+BEM (fine) for frequency range 300-400 Hz.*

## Computation cost

The direct FWH method required about 40 CPU-hours, while the FWH+BEM method took 1460 (coarse) and 7050 (fine) CPU-hours. The scalability of both methods has been tested and both solvers exhibit close to linear scaling up to 1600 cores for the present case.
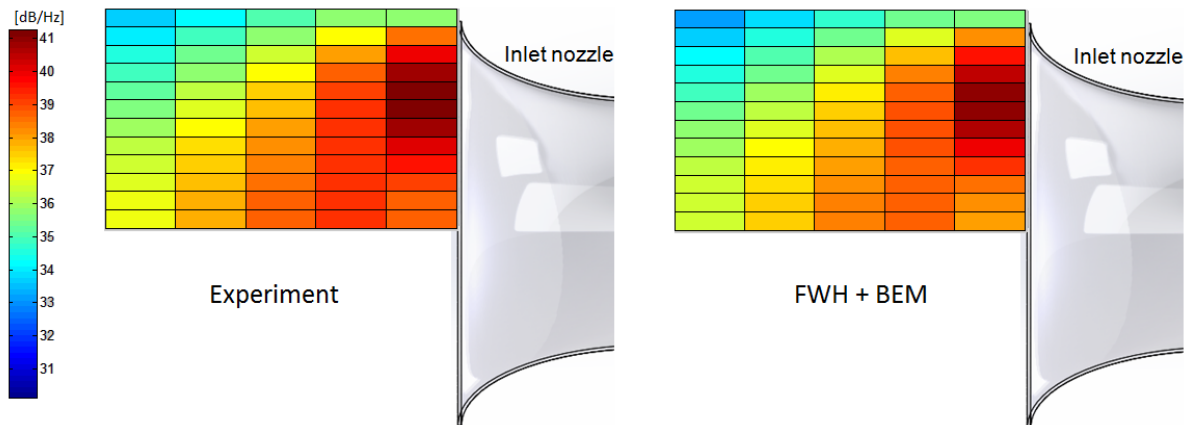


*Figure 9: Comparison of color maps from experiment and LES+BEM (fine) for frequency range 500-600 Hz.*
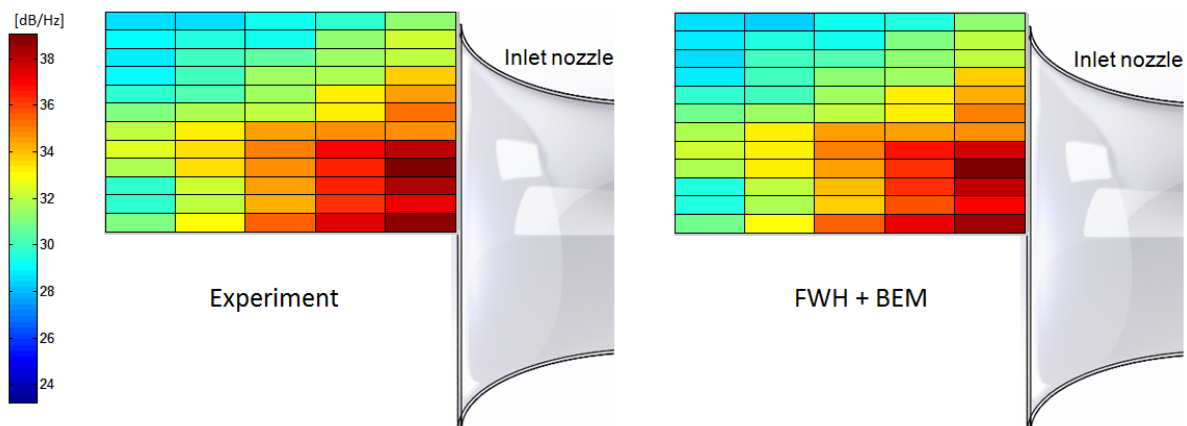


*Figure 10: Comparison of color maps from experiment and LES+BEM (fine) for frequency range 3000-3300 Hz.*

The computational cost of the direct FWH and FWH+BEM methods differs significantly, as should be expected. While the direct FWH method involves only integration over the FWH surface panels with a kernel represented by a Green's function and thus can be effectively parallelized, the FWH+BEM method involves solution of large number of complex dense matrix systems – one system per frequency with the matrix size of $N{\times}N$ where $N$ is the number of BEM panels – which is a very expensive calculation. To speed up the code, the solution of linear systems was performed using a parallel linear solver from ScaLAPACK [13] taken from the Intel Math Kernel Library. While this constitutes a plausible solution, because the computational effort for the whole fan noise modeling is still dominated by the cost of Large Eddy Simulation of the fan flow, the BEM solver can still use some improvement. As current research shows, a dramatic speedup of the linear system solver is possible with the help of hierarchically off-diagonal low-rank matrices [14,15]. These future advancements are expected to make it feasible for the FWH+BEM method to be employed in environment where a fast turnaround is required, e.g., a product design process.

# CONCLUSIONS AND PERSPECTIVES

A high-fidelity method for noise propagation has been developed and implemented in a massively parallel LES framework. The method takes an input from an LES simulation of a flow in a particular component and propagates the acoustic waves to a specified location. The method is able to compute flow-borne noise in complex geometries due to its ability to account for reflections from hard surfaces of arbitrary shape. A validation study has been performed using acoustic and flow data for the case of an automotive cooling fan. The resulting noise spectra are found to follow closely the experimental results. Also the validation results show that even in relatively simple geometries, such as a fan in a pipe, the sound reflections play an important role in overall noise level and thus cannot be discarded during the analysis.

The method is highly scalable and is targeted towards the HPC environment. With the decreasing costs of computation and increasing availability of massively parallel computers we expect that it will be feasible in the near future to incorporate the combination of LES for flow simulation and FHW+BEM method for noise propagation into the product development process for industrial components.

# BIBLIOGRAPHY

[1] SG Chumakov, ST Bose, FE Ham – *Efficient Large-Eddy Simulation of a low-Mach number axial fan.* FAN2015 Conference (submitted), **2015**

[2] K Sampath, J Katz – *Phase locked PIV measurements in wake of an automotive fan model.* FAN2015 Conference (submitted), **2015**

[3] JE Ffowcs Williams, DL Hawkings – *Sound generation by turbulence and surfaces in arbitrary motion*. Phil. Trans. Ryo. Soc., A264, **1969**

[4] DP Lockard – *An efficient, two-dimensional implementation of the Ffowcs Williams and Hawkings equation*. J. Sound. Vib, Vol. 229, pp. 897-911, **2000**

[5] GA Brès, JW Nichols, SK Lele, F Ham – *Towards best practices for jet noise predictions with unstructured large eddy simulations*. AIAA paper 2012-2965, **2012**

[6] A Pilon, A Lyrintzis – *An improved Kirchhoff method for jet aeroacoustics,* AIAA paper 96-1709, **1996**

[7] KS Brentner, F Farassat – *Analytical comparison of the acoustic analogy and Kirchhoff formulation for moving surfaces,* AIAA Journal 36(8), pp.1379-1386, **1998**

[8] MJ Lighthill – *On sound generated aerodynamically, I: General Theory,* Proceedings of the Royal Society, A221, pp.564-587, **1952**

[9] Y Khalighi, A Mani, FE Ham, P Moin – *Prediction of Sound Generated by Complex Flows at Low Mach Numbers*. AIAA Journal Vol. 48, no. 2, **2010**

[10] MB Giles – *Nonreflecting Boundary Conditions for Euler Equation Calculations.* AIAA Journal Vol. 28, no. 12, **1990**

[11] T Colonius, SK Lele, P Moin – *Boundary conditions for direct computation of aerodynamic sound generation*. AIAA Journal Vol. 31, no. 9, **1993**

[12] A Mani – *Analysis and Optimization of Numerical Sponge Layers as a Nonreflective Boundary Treatment.* Journal of Computational Physics Vol. 231, no. 2, **2012**

[13] http://ww.netlib.org/scalapack

[14] S Ambikasaran, E Darve – *A O(N log N) fast direct solver for partial hierarchically semi-separable matrices,* J. Sci Comput, 57:477-501, **2013**

[15] A Aminfar, S Ambikasaran, E Darve – *A fast block low-rank dense solver with applications to finite-element matrices*, arXiv preprint arXiv:1403.5337, **2014**